論文 / 著書情報
Article / Book Information

Title	Fabrication of CoFeB–SiO2 Films With Large Uniaxial Anisotropy by Facing Target Sputtering and its Application to High-Frequency Planar-Type Spiral Inductors
Authors	Y. Takamura, H. Nitta, K. Kawahara, T. Kaneko, R. Ishido, T. Miyazaki, N. Hosoda, K. Fujisaki, S. Nakagawa
Citation	IEEE Transactions on Magnetics, Vol. 59, Issue 11, pp. 1-4
Pub. date	2023, 7
Copyright	(c) 2023 IEEE. Personal use of this material is permitted. Permission from IEEE must be obtained for all other uses, in any current or future media, including reprinting/republishing this material for advertising or promotional purposes, creating new collective works, for resale or redistribution to servers or lists, or reuse of any copyrighted component of this work in other works.
DOI	http://dx.doi.org/10.1109/TMAG.2023.3291879
Note	This file is author (final) version.

This article has been accepted for publication in IEEE Transactions on Magnetics. This is the author's version which has not been fully edited and content may change prior to final publication. Citation information: DOI 10.1109/TMAG.2023.3291879

Fabrication of CoFeB-SiO_2 Films with Large Uniaxial Anisotropic by Facing Target Sputtering and its Application to High Frequency Planar Type Spiral Inductors

Yota Takamura[1], Member, *IEEE*, Honami Nitta[1], Kazuma Kawahara[1], Tadayuki Kaneko[1], Ryosuke Ishido[2]
Tatsuya Miyazaki[2], Naoki Hosoda[3], Keisuke Fujisaki[3], Member, *IEEE*, Shigeki Nakagawa[1], Member, *IEEE*

[1]School of Engineering, Tokyo Institute of Technology, Meguro, Tokyo, 152-8553, Japan
[2]ROHM Co., Ltd., Kyoto, Kyoto 615-8585, Japan
[3]Toyota Technological Institute, Nagoya, Aichi, 468-0034, Japan

A comprehensive study on fabrication of CoFeB-SiO_2 films with large in-plane magnetic anisotropy for the use in high frequency inductors in power electronics circuits was conducted. The magnetic films were deposited using facing target sputtering which can introduce large uniaxial magnetic anisotropy in the plane. A multilayer structure consisting of CoFeB-SiO_2 and SiO_2 layers suppressed columnar growth and thus reduced undesired perpendicular magnetic anisotropy. As a result, a 1 µm thick magnetic layer was achieved with excellent soft magnetic properties and no stripe domain structure. The effectiveness of these magnetic films was demonstrated by fabricating and characterizing planar type spiral coils. This development of micro magnetic inductors using the magnetic layer shows great potential for use in high frequency power electronics applications.

***Index Terms*—Soft magnetic materials, nano granular, micromagnetic inductors, high frequency power electronics**

I. Introduction

Recent development in power semiconductor devices such as SiC and GaN power transistors has opened the use of high frequency in operation of power electronics circuits, e.g. dc-dc converters [1]. Rising the operation frequency has contributed to increasing the power conversion efficiency and shrinking the volume of component devices.

Micromagnetic inductors, which is magnetic inductor fabricated with semiconductor manufacturing processes, are very promising to make a small size and low heigh devices [2]. Many researches in the micromagnetic inductors have been conducted until 2000s [2]–[4] and the importance has increased as the operation frequency of the semiconductor devices becomes higher [5].

Soft magnetic nano granular films are attractive as high frequency magnetic materials for micromagnetic inductors. In this study we chose CoFeB-SiO_2 granular [6], [7] which consists of CoFeB granules with large saturation magnetization embedded in electrical insulating SiO_2 matrix. Thanks to the electrical insulating matrix, CoFeB-SiO_2 nano granular exhibits high electrical resistivity and thus they show low eddy current loss at high frequency operation, which is further important at higher frequency operation. It is note that no thermal runaway [8] occurs in nano granular unlike ferrites .

Large magnetic anisotropic films are attractive as the magnetic cores since the hysteresis loss along its hard axis can be lowered [9]. Moreover, magnetic dynamics along the hard axis consider to be magnetic rotation in majority, which can follow higher frequency magnetic field than magnetic domain motion.

We have demonstrated that facing target sputtering (FTS) method can form significant magnetic anisotropy in singular phase CoFeB films, resulting in low hysteresis loss in the hard axis direction [10], [11]. This induced magnetic anisotropy is formed mainly due to the oblique incidence of sputtered particles.

In this study we successfully formed large magnetic anisotropy in nano-granular CoFeB-SiO_2 films, and demonstrated multilayers of CoFeB-SiO_2 and SiO_2 exhibited such soft-magnetic properties. Further, we developed a planar type spiral inductor with it and successfully operated it.

II. Preparation and Characterization of High Anisotropic CoFeB-SiO_2 Film

A. Fabrication

CoFeB-SiO_2 films were deposited on thermally oxidized Si substrates using the FTS technique with an RF power supply as

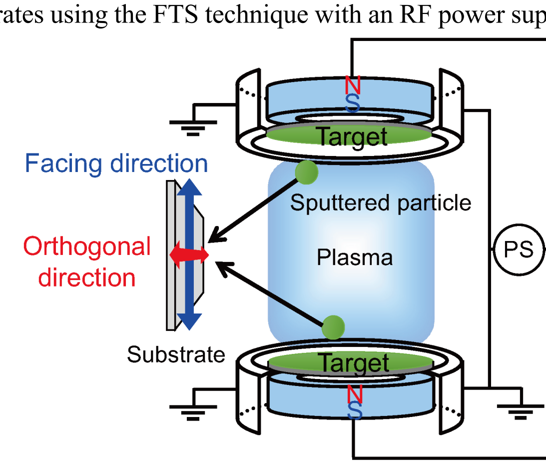

FIG. 1 Facing target sputtering with a rf power supply.

Manuscript received April 1, 2015; revised May 15, 2015 and June 1, 2015; accepted July 1, 2015. Date of publication July 10, 2015; date of current version July 31, 2015. Corresponding author: Y. Takamura (e-mail: takamura@ee.e.titech.ac.jp).

Color versions of one or more of the figures in this paper are available online at http://ieeexplore.ieee.org.

Digital Object Identifier (inserted by IEEE).

This article has been accepted for publication in IEEE Transactions on Magnetics. This is the author's version which has not been fully edited and content may change prior to final publication. Citation information: DOI 10.1109/TMAG.2023.3291879

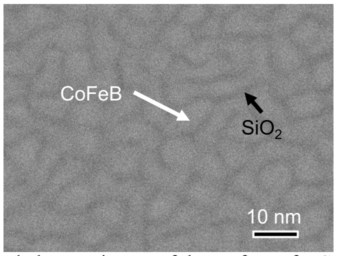

FIG. 2 Back scattered electron image of the surface of a $CoFeB-SiO_2$ film.

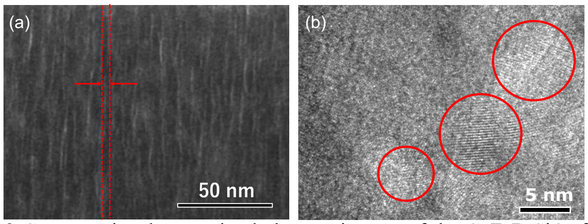

FIG. 3 Cross sectional transmitted electron images of the $CoFeB-SiO_2$ film. (a) Wide range view and (b) magnified view.

shown in Fig. 1. The sputtering targets were composed of $Co_{66.4}Fe_{7.6}B_{26}$ and SiO_2 in a ratio of 80:20 in mol%. Ar gas was used as sputtering gas and the total pressure was fixed at 0.5 Pa. The deposition rate was set at 1.7 nm/min. The substrate temperature was maintained at ambient temperature without cooling with water. SiO_2 layers in multilayer were formed from the other SiO_2 targets in the same sputtering chamber.

B. Characterization

Firstly, we analyzed structural properties of a single $CoFeB-SiO_2$ layer. Fig. 2(a) show a backscattered electron images of a $CoFeB-SiO_2$ film observed using a second electron microscope. The image contrast reveled the phase separation of CoFeB and SiO_2. The grain size of CoFeB granules was approximately 6 nm. In Fig. 3, we present cross-sectional transmission electron microscopy images with the vertical direction corresponding to the growth direction of the film. As shown in. Fig. 3(a), the streak patterns, with widths ranging from 3.5 nm to 6 nm, indicate the formation of a columnar structure. Fig. 3(b) shows a magnified view of a CoFeB granule. Some areas show lattice images, while others exhibit an amorphous-like structure. This indicates that both nano-crystal and amorphous structures coexisted in the $CoFeB-SiO_2$ film.

Fig. 4 shows magnetization, I, vs magnetic field, H, curves for various $CoFeB-SiO_2$ single layer thickness, ranging from 10 nm to 1050 nm. The measurements were conducted using a vibrating magnetometer. Within a thickness range between 90 nm and 200 nm, the samples exhibited excellent soft-magnetic properties with large magnetic anisotropy and a closed hysteresis loop along their hard axes. The hard and easy axis was formed along facing and orthogonal direction in the plane, respectively. The samples with thickness less than 50 nm showed slightly opened hysteresis loops for their hard axis, suggesting the initial growth of $CoFeB-SiO_2$ from the substrates was different from that of the thicker region. For samples thicker than 250 nm, the I-H loops were opened for the both directions, and are typical characteristics when a stripe domain structure forms [10]. The stripe domain can be caused by a combination of in-plane and perpendicular magnetic anisotropy (PMA) which could originate from the shape magnetic anisotropy of columnar structures observed in the TEM images.

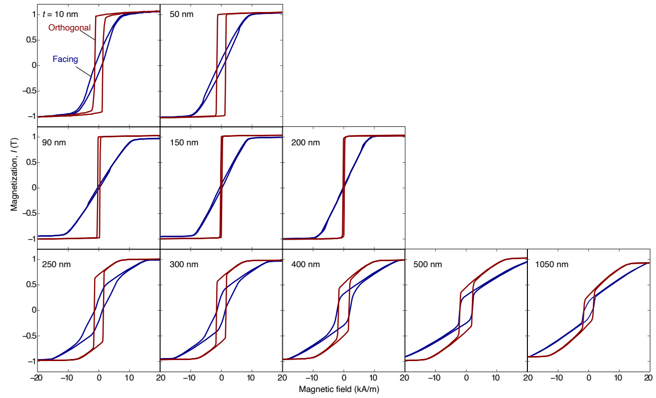

FIG. 4 Magnetization (I) versus field curves for $CoFeB-SiO_2$ single layers with various thickness.

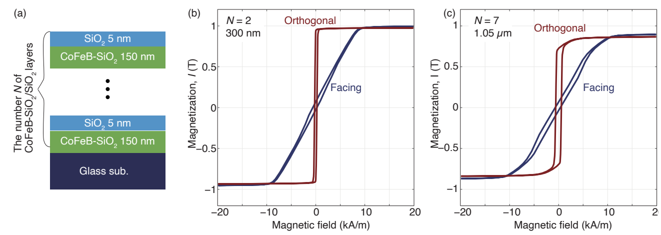

FIG. 5 (a) Structure of multilayered $CoFeB-SiO_2$ and SiO_2 layers. (b) and (c) I-H curves for multilayered films with the repetition number N = 2 and 7, respectively.

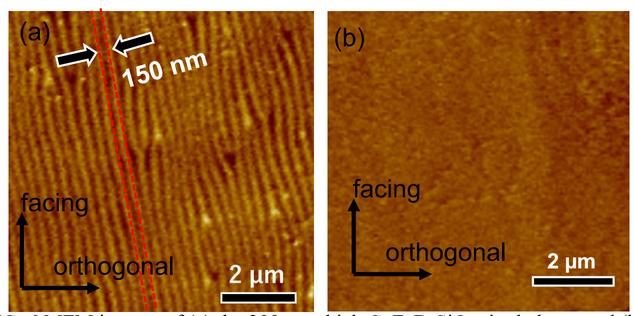

FIG. 6 MFM images of (a) the 300 nm-thick $CoFeB-SiO_2$ single layer and (b) $[CoFeB-SiO_2/SiO_2]_2$ layer. The total $CoFeB-SiO_2$ thickness was 300 nm in both films.

To achieve thicker films with soft magnetic properties, we fabricated multilayers composed of 150 nm-thick $CoFeB-SiO_2$ layers and 5 nm-thick SiO_2 layer as illustrated in Fig. 5 (a). The repetition number N varied from 2 to 7. The inserted SiO_2 layer can lower the height of the nanocolumns of $CoFeB-SiO_2$ to reduce shape anisotropy and thus PMA. The resulting magnetic properties for $N = 2$ and $N = 7$ were shown in Fig. 5(b) and 5(c), respectively. Compared to the single layers with the same thickness, the multilayers exhibited significantly improved soft-magnetic properties. Even in a multilayer with a total $CoFeB-SiO_2$ thickness of 1 μm (N = 7), soft-magnetic properties were maintained, as shown in Fig. 5(b). Thinning the $CoFeB-SiO_2$ layer to 100 nm and increasing N to 10 resulted in an improved the squareness ratio.

To confirm the formation of stripe domain structures in the single layer and its suppression in the multilayer, we performed magnetic force microscopy (MFM) measurements. Fig. 6 shows MFM images of (a) the 300 nm-thick single layer and (b) mutlilayers with $N = 2$. Note that the total thickness of $CoFeB-SiO_2$ layers was the same in the both films. After the samples

This article has been accepted for publication in IEEE Transactions on Magnetics. This is the author's version which has not been fully edited and content may change prior to final publication. Citation information: DOI 10.1109/TMAG.2023.3291879

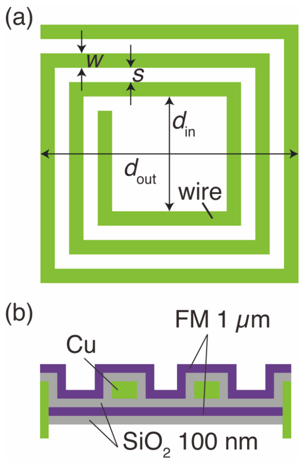

FIG. 7 Schematics device structure used for simulation. (a) planer and (b) cross sectional structure.

TABLE I
PARAMETERS FOR SIMULATION

Symbol	Quantity	Value
d_{m}	Inner size	2.6 mm
d_{out}	Outer size	9.0 mm
w	Wire width	0.25 mm
S	Space	0.1 mm
n	The number of turns	6

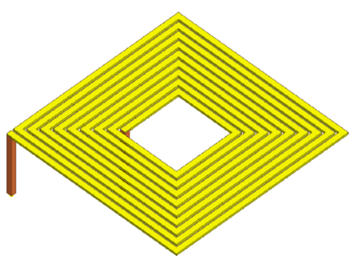

FIG. 8 Generated structure of a spiral coil in FEMMET.

were magnetized along the facing direction with a field of 20 kA/m, the MFM images were captured in a remanent state under the zero magnetic field. As shown in Fig. 6(a), clear stripe domain structures were observed, with a domain width of approximately 150 nm. The directions of the stripe domains were random, in regardless of facing and orthogonal directions. On the other hand, a single magnetic domain structure was observed in the multilayers in Fig. 6(b). Both results were consistent with the dc magnetic analysis in Figs. 4 and 5.

The high freuqncy permeability of the mutlilayere with $N = 7$ were measrued. The ferromagnetic resonance was obsreved at the frequency of 2 GHz, which is consistent with the estimated value from the Kittel's formula using saturaiton magentization, 1.1 T, and anisotropic field, 8.5 kA/m, obtained from the dc magnetic properties. Note that fitting of the measured permeability versus freuqnecy curves give a results of low damping factor of 0.01.

The electrical resistivities for the single layers and multilayerse were measured with the four probe method. In single layers, the resisstivity increased in thin layer and then becomes constant at approximately 400 μΩ cm in the samples thickner than 150 nm. The results implieds the initial layer had a different structure, which agrees with the dc magnetic

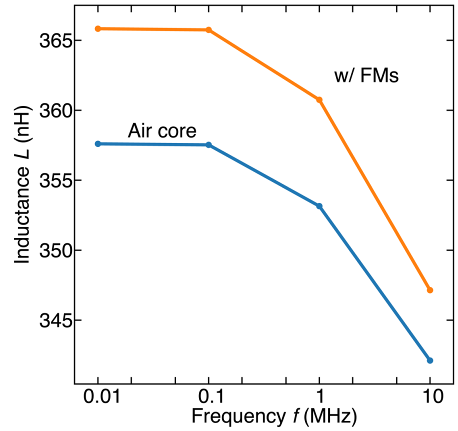

FIG. 9 Simulation results

proeprties for thin samples. The resistivity in multilayers were roughly the same as that of the 150 nm-thick single layer, which agrees with as previously reports [11]. Although the average resistivity did not increase to the repetition number, the formation of multilayers contributes to reducing eddy current loss by suppressing electrical current flow in the direction perpendicular to the layers.

Summarizing this part, we successfully fabricated soft magnetic 1 μm-thick ferromagnetic layers consisting of CoFeB-SiO_2 and SiO_2 multilayers as a magnetic core for spiral inductors. Saturation magnetization and anisotropic filed were approximately 1.1 T and 8.5 kA/m, respectively. The relative permeability was determined to be approximately 100.

III. SPIRAL COIL INDUCTOR

A. Simulation

A planar spiral coil was designed and simulated with FEMTET developed by Murata Software [12]. Schematic device structure for planer and cross-sectional views were illustrated in Fig. 7(a) and 7(b), respectively. In simulation, two magnetic layers with 1 μm thick were placed on top and bottom of a Cu coil via electrically insulating SiO_2 layers. TABLE I summarizes the parameters used in the FEM calculations. Fig. 8 shows a inductor structure that was generated using FEMTET. The frequency range for this calculation is 10 kHz to 10 MHz.

Fig. 9 shows simulated inductance L as a function operation frequency f for air coil and coil with two ferromagnetic (FM) layers. L increases by 5 % by depositing CoFeB-SiO_2 layer for the top and bottom of the coil. The increase of L is not significant because the thickness of the FM layers is thin compared to the distribution of magnetic flux that leaks into air part below/above the FM layers. While increasing the FM thickness could further enhance L, we selected 1 μm as a practical thickness achievable with sputtering deposition technique. L slightly decreases with increasing frequency f due to the eddy currents in the wire owing to the skin effect [13].

B. Fabrication

We fabricated planar type spiral inductors with a [CoFeB-SiO_2(100 nm)/SiO_2(5 nm)]$_{10}$ multilayer on a thermally oxidized Si substrate. After depositing the multilayers, we formed a 100 nm-thick SiO_2 layer to insulate between the magnetic core and

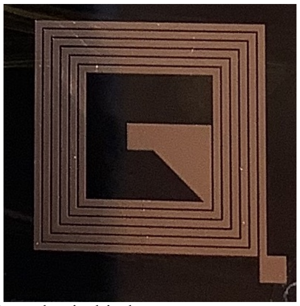

FIG. 10 Photo of fabricated spiral inductors.

coil layer. We then deposited seed layers of Cr and Cu, followed by photolithography to pattern a thick photo resist (La900, Tokyo Ohka Kogyo). Next, a 12 µm-thick Cu was electrically plated as a coil [14]. After removing the photoresist, we completely etched the seed layer with Ar ion milling. Fig. 10 shows a photo of the fabricated inductor with 9 mm x 9 mm footprint. In the experiment, we did not deposit top magnetic layer. As a reference, we also fabricated an air core coil with the same dimensions.

C. Characterization and discussion

Inductance L of the spiral inductor was measured with an impedance analyzer. Fig. 11shows L as a function of frequency f. The parasitic impedance was eliminated from the data by subtracting the impedance of a dummy sample. The inductance of the spiral coil with the magnetic core was found to be larger than that of the air core, due to the contribution of the magnetic core.

On comparing the simulation and experimental results, it was found that even in the results of air core did not completely match. Further, the enhancement of L by adding magnetic cores were higher in experimental. The dimensions fabricated in the inductors might not be the exact same as designed.

Finally, we would like to discuss the resonance occurred at 3.6 MHz in the spiral coil with a magnetic core, which can convert to a few nF. This could be caused by a parasitic capacity in the spiral inductor, most likely due to the capacitance between the ferromagnetic layer and coils separated by 100 nm-thick SiO_2 layer as the calculated capacitance using the parallel plate approximation well matched the experimental results [15]. We should note that the resonance occurred at a much lower frequency than the ferromagnetic frequency of the CoFeB-SiO_2 multilayers.

IV. CONCLUSION

A comprehensive study ranging from fabrication of soft-magnetic CoFeB-SiO_2 films with large magnetic anisotropy in the plane by with FTS to simulation, and device operation of integrated inductors were conducted. We successfully demonstrated planar type spiral coils with magnetic cores formed with facing targe sputtering for high frequency power electronics. Further studies on the inductors will be needed to characterize material in high frequency.

ACKNOWLEDGMENT

This work was supported by the ROHM Co., Ltd. and power academy. The authors thank to Prof. Y. Kagohashi, Tokyo Inst. of Tech. for his support of this project. The authors thank Prof.

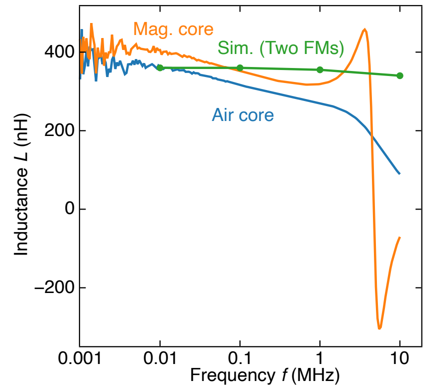

FIG. 11 Inductance of fabricated spiral inductors.

M. Yamaguchi and Mr. Y. Miyazawa, Tohoku Univ., and Prof. M. Saito, Waseda Univ.. We also thank Materials Analysis Division and electronic material characterization equipment sharing promotion group, Open Facility Center, Tokyo Inst. of Tech.. This work was supported by "Advanced Research Infrastructure for Materials and Nanotechnology in Japan (ARIM)" of the Ministry of Education, Culture, Sports, Science and Technology (MEXT). Proposal Number JPMXP1222WS018.

REFERENCES

[1] K. Fujisaki, “Magnetic Material Excited by Power Electronics in Electrical Engineering,” presented at the TMS2017 46th Annual Meeting & Exhibition, Sandiego, California, USA, Mar. 01, 2017.

[2] T. Sato, H. Tomita, A. Sawabe, T. Inoue, T. Mizoguchi, and M. Sahashi, “A magnetic thin film inductor and its application to a MHz switching dc-dc converter,” *IEEE Trans. Magn.*, vol. 30, no. 2, pp. 217–223, Mar. 1994, doi: 10.1109/20.312261.

[3] M. Yamaguchi, K. Yamada, and K. H. Kim, “Slit Design Consideration on the Ferromagnetic RF Integrated Inductor,” *IEEE Trans. Magn.*, vol. 42, no. 10, pp. 3341–3343, Oct. 2006, doi: 10.1109/TMAG.2006.879636.

[4] D. S. Gardner *et al.*, “Integrated On-Chip Inductors with Magnetic Films,” in *2006 International Electron Devices Meeting*, San Francisco, CA, USA: IEEE, 2006, pp. 1–4. doi: 10.1109/IEDM.2006.347002.

[5] D. V. Harburg *et al.*, “Microfabricated Racetrack Inductors With Thin-Film Magnetic Cores for On-Chip Power Conversion,” *IEEE J. Emerg. Sel. Topics Power Electron.*, vol. 6, no. 3, pp. 1280–1294, Sep. 2018, doi: 10.1109/JESTPE.2018.2808375.

[6] M. Munakata *et al.*, “Drastically Increased Electrical Resistivity of a (CoFeB)-SiO2 Magnetic Thin-Film Core in a Small GHz Range.,” *J. Magn. Soc. Jpn.*, vol. 26, no. 4, pp. 509–512, 2002, doi: 10.3379/jmsjmag.26.509.

[7] T. Eguchi, N. Nakagawa, M. Yonetsu, K. Okamoto, T. Suetsuna, and S. Suenaga, “High-frequency magnetic properties of (FeCoNbB)-(SiO2) nanocolumnar films,” *J. Appl. Phys.*, vol. 115, no. 17, p. 17A311, May 2014, doi: 10.1063/1.4863166.

[8] F. Farahmand, F. P. Dawson, and J. D. Lavers, “Critical Temperature for Thermal Runaway in a Magnetic Material,” *IEEE Trans. Magn.*, vol. 44, no. 11, pp. 4513–4516, Nov. 2008, doi: 10.1109/TMAG.2008.2003399.

[9] M. Sonehara, K. Ikeda, and T. Sato, “Control of Magnetic Moment in Uniaxial Anisotropy Magnetic Thin Film Taking Leakage Flux in RF Planar Spiral Inductors with Closed-Magnetic Core into Account,” *Electr Eng Jpn*, vol. 191, no. 2, pp. 1–6, Apr. 2015, doi: 10.1002/eej.22693.

[10] Y. Cao, Y. Zhang, S. Ohnuma, N. Kobayashi, and H. Masumoto, “Structure and Isotropic High-Frequency Response of Co-HfN Nanogranular Films,” *IEEE Trans. Magn.*, vol. 51, no. 11, pp. 1–4, Nov. 2015, doi: 10.1109/TMAG.2015.2438003.

[11] M. Munakata *et al.*, “Thickness effect on 1 GHz permeability of (CoFeB)-(SiO2) films with high electrical resistivity,” *IEEE Trans. Magn.*, vol. 37, no. 4, pp. 2258–2260, Jul. 2001, doi: 10.1109/20.951141.

[12] “FEMTET.” Murata Software Co., Ltd, 2023. [Online]. Available: https://www.muratasoftware.com/en/

[13] N. Klemmer, "Inductance calculations for MCM system design and simulation," in *Proceedings of 1995 IEEE Multi-Chip Module Conference (MCMC-95)*, Santa Cruz, CA, USA: IEEE Comput. Soc. Press, 1994, pp. 81–86. doi: 10.1109/MCMC.1995.512008.

[14] K. Uda *et al.*, "Fabrication of Π-structured Bi-Te thermoelectric micro-device by electrodeposition," *Electrochimica Acta*, vol. 153, pp. 515–522, Jan. 2015, doi: 10.1016/j.electacta.2014.12.019.

[15] C. P. Yue and S. S. Wong, "Physical modeling of spiral inductors on silicon," *IEEE Trans. Electron Devices*, vol. 47, no. 3, pp. 560–568, Mar. 2000, doi: 10.1109/16.824729.